Structure of Extended Lipopolysaccharide Glycoforms Containing Two Globotriose Units in *Haemophilus influenzae* Serotype b Strain RM7004‡

Hussein Masoud,[§,||] Adèle Martin,[§] Pierre Thibault,[§] E. Richard Moxon,[⊥] and James C. Richards*[,§]

Institute for Biological Sciences, National Research Council of Canada, Ottawa, Ontario K1A 0R6, Canada, Department of Biological Sciences, Faculty of Science, University of Jordan, Amman, Jordan, and Molecular Infectious Diseases Group and Department of Paediatrics, Institute for Molecular Medicine, John Radcliffe Hospital, Headington, Oxford 0X3 3DU, United Kingdom

Received August 14, 2002; Revised Manuscript Received January 24, 2003

ABSTRACT: Lipopolysaccharide (LPS) is a major virulence determinant of the human bacterial pathogen *Haemophilus influenzae*. Structural elucidation of the LPS from *H. influenzae* type b strain RM7004 was achieved by using electrospray ionization mass spectrometry (ESI-MS) and high-field NMR techniques on delipidated LPS and core oligosaccharide samples of LPS. It was found that the organism elaborates a series of related LPS glycoforms having a common inner-core structure, but differing in the number and position of attached hexose residues. LPS glycoforms containing between four and nine hexose residues were structurally characterized. The inner-core element was determined to be L-α-D-Hep*p*-(1→2)-[PEA→6]-L-α-D-Hep*p*-(1→3)-[*β*-D-Glc*p*-(1→4)]-L-α-D-Hep*p*-(1→5)-[P→4]-α-KDO*p*-(2→, a structural feature which has been identified in every *H. influenzae* strain investigated to date. Two major groups of isomeric glycoforms were characterized in which the terminal Hep*p* residue of the inner-core element was either substituted at the O-2 position with a *β*-D-Gal*p* residue or not. The structures of the major LPS glycoforms were found to have oligosaccharide chain extensions from O-3 of the middle Hep*p* residue. Glycoforms containing five and six hexose residues were most abundant and were shown to carry the tetrasaccharide unit α-D-Gal*p*-(1→4)-*β*-D-Gal*p*-(1→4)-*β*-D-Glc*p*-(1→4)-α-D-Glc*p* at the O-3 position of the middle heptose. This tetrasaccharide displays the globoside trisaccharide (globotriose) as a terminal epitope, a structure that is found on many human cells (P^k blood group antigen) and which is thought to be an important virulence determinant for *H. influenzae*. LPS glycoforms were characterized that had further chain extension from the *β*-D-Glc*p*-(1→ residue of the proximal Hep*p*. In the fully extended LPS (Hex9/Hex8′ glycoforms), both the proximal and middle heptose residues carried tetrasaccharide chains displaying terminal globotriose epitopes. In addition, the LPS was found to carry phosphorylcholine and *O*-acetyl groups.

Haemophilus influenzae remains a significant cause of disease worldwide. Both capsular and acapsular (nontypable) strains are recognized, and the potential of this pathogen to cause disease has been linked to its ability to express capsular polysaccharide (*1*) and lipopolysaccharide (LPS)[1] (*2*) epitopes. Strains belonging to capsule serotype b are most invasive (*3*, *4*). LPS is an essential and characteristic surface component of *H. influenzae*. This group of bacteria has been found to express heterogeneous populations of short-chain LPS that display extensive structural and antigenic diversity among multiple oligosaccharide epitopes. Recent studies have firmly established that LPS of *H. influenzae* is comprised of a conserved inner-core triheptosyl unit that is attached to a lipid A moiety via 3-deoxy-D-*manno*-octulosonic acid (KDO) 4-phosphate (*5*, *6*). The inner-core unit provides the template for attachment of oligosaccharide- and non-carbohydrate-containing substituents, of which the nature and substitution patterns can vary both within and between strains (*6*−*10*). *H. influenzae* LPS has been found to mimic host surface antigens (*11*) and has the propensity for reversible switching of terminal oligosaccharide epitopes, a process known as phase variation (*12*, *13*). The underlying genetic mechanism of phase variation is well-documented (*14*). Gene functions have been identified that are responsible for many of the steps involved in LPS oligosaccharide biosynthesis in type b strain Eagan (*15*) and in the genome-sequenced strain, Rd (*16*, *17*). In our laboratories, we have been interested in the genetic and molecular aspects of expression of the globotriose epitope [α-D-Gal*p*-(1→4)-*β*-D-Gal*p*-(1→4)-*β*-D-Glc*p*] in *H. influenzae* LPS (*7*, *8*, *15*, *17*−*19*). This epitope is found on many human cells, for example, as a component of the globo series of glycolipids (blood group P^k antigen), structures implicated as receptors for bacterial ligands (*18*, *20*). In the

‡ National Research Council of Canada Publication 42469.

* To whom correspondence should be addressed: Institute for Biological Sciences, National Research Council of Canada, Ottawa, ON K1A 0R6, Canada. Telephone: (613) 990-0854. Fax: (613) 941-1327. E-mail: Jim.Richards@nrc.ca.

§ National Research Council of Canada.

|| University of Jordan.

⊥ John Radcliffe Hospital.

[1] Abbreviations: DOC−PAGE, deoxycholate−polyacrylamide gel electrophoresis; GLC−MS, gas liquid chromatography−mass spectrometry; ESI-MS, electrospray ionization mass spectrometry; CZE, capillary zone electrophoresis; COSY, correlated spectroscopy; TOCSY, total correlated spectroscopy; HMQC, heteronuclear multiple-quantum coherence; NOE, nuclear Overhauser effect; NOESY, two-dimensional NOE spectroscopy; KDO, 3-deoxy-D-*manno*-octulsonic acid; LPS, lipopolysaccharide; LPS-OH, O-deacylated LPS; OS, oligosaccharide; PEA, phosphoethanolamine; PPEA, pyrophosphoethanolamine; KDO, 3-deoxy-D-*manno*-octulosonic acid.

10.1021/bi026632a CCC: $25.00
Published on Web 03/28/2003

type b strain Eagan, the globotriose epitope is expressed as a terminal trisaccharide moiety of a tetrasaccharide extension from the central heptose of the LPS inner-core unit (*7*). In the type d-derived strain, Rd, the globotriose epitope is expressed in a different molecular environment, being present as a trisaccharide extension from the distal heptose of the inner-core unit (*8*). It is noteworthy that the glycosyltransferases involved in the biosynthesis of this trisaccharide unit are encoded by homologous genes in the two strains (*17*). In the investigation presented here, we provide evidence that type b strain RM7004 elaborates LPS having a basal structure similar to that of strain Eagan, but displaying the capacity to express simultaneously two globotriose units on chain extensions from the proximal and middle heptose residues of the inner-core unit in fully assembled glycoforms.

EXPERIMENTAL PROCEDURES

Bacterial Growth and LPS Preparation. H. influenzae type b strain RM7004 was obtained from the culture collection of E. R. Moxon (Oxford University, Oxford, U.K.). This strain was originally obtained from L. van Alphen (strain 760705), one of several isolates from invasive diseases in The Netherlands (*21*). Bacteria were cultivated in liquid media of brain heart infusion broth as described elsewhere (*7*). Cell pellets obtained by centrifugation of the bacterial culture were washed, successively, once with ethanol, twice with acetone, and twice with petroleum ether (35−60 °C). The LPS was extracted from the air-dried cellular material by the hot phenol−water procedure (*22*), followed by extensive dialysis, or by precipitation with 4 volumes of ethanol (*7*). Crude LPS was purified by repeated ultracentrifugation (105000*g* at 4 °C for 5 h).

Deoxycholate−Polyacrylamide Gel Electrophoresis (DOC−PAGE). PAGE was performed using the buffer system of Laemmli and Favre (*23*) as modified by Komuro and Galanos (*24*) with DOC as the detergent. LPS bands were visualized with a silver staining procedure as described by Tsai and Frasch (*25*).

Oligosaccharide Preparation. O-Deacylated LPS, LPS backbone oligosaccharide, and core OS were prepared as described previously (*7*, *26*−*28*). The backbone OS products were fractionated on the Bio-Gel P2 gel filtration column (2.6 cm × 140 cm, 200−400 mesh, Bio-Rad). Elution was performed with pyridinium acetate (0.05 M, pH 4.5). Column eluants were continuously monitored for changes in refractive index with a Waters R403 differential refractometer, and collected fractions (4.5 mL) were assayed colorimetrically for neutral glycoses by the phenol−sulfuric acid method (*29*).

Analytical Methods and Methylation Analysis. Glycoses were identified by GLC as their alditol acetate derivatives. Samples (0.2−0.5 mg) were hydrolyzed with 2 M TFA for 90 min at 125 °C and evaporated to dryness under a stream of nitrogen. The liberated glycoses were reduced ($NaBH_4$) and acetylated (Ac_2O) as previously described (*30*). Peracetylated heptitol derivatives were found to be the L-*glycero*-D-*manno* (or D-*glycero*-L-*manno*) configuration by comparison of their GLC retention times with that of an authentic standard. The L-*glycero*-D-*manno* absolute stereochemistry is assumed on biosynthetic grounds (*31*). The stereochemistry of the hexoses was established to be the D-configuration by GLC analysis of their acetylated (*R*)-2-octyl glycoside derivatives (*32*). The KDO residues in *H. influenzae* LPS were previously reported to have the D-*manno* absolute configuration (*33*). GLC analysis was performed with a Hewlett-Packard model 5890 series II gas chromatograph fitted with a hydrogen-flame ionization detector, using a fused-silica capillary column (0.3 mm × 25 m) containing 3% OV 17; an initial column temperature of 180 °C was held for 2 min, followed by an increase to 240 °C at a rate of 2 °C/min. Methylation analysis was performed on an LPS backbone OS sample (∼2 mg) with iodomethane in dimethyl sulfoxide containing an excess of potassium (methylsulfinyl) methanide (*34*). Excess iodomethane was evaporated under a stream of nitrogen; water (3 mL) was added, and the methylated oligosaccharides were purified on a Sep-Pak C-18 cartridge as previously described (*35*). Purified methylated oligosaccharide was hydrolyzed with 0.25 M H_2SO_4 in 95% acetic acid at 85 °C overnight, reduced ($NaBD_4$), and acetylated according to acetolysis procedure of Stellner et al. (*36*). Partially methylated alditol acetates were separated by GLC and identified by electron impact (EI-MS) on a Varian Saturn Iontrap GLC−MS system fitted with a DB-17 fused-silica capillary column (0.25 mm × 25 m), using the temperature program which began at 180 °C for 2 min followed by an increase to 320 °C at a rate of 5 °C/min.

NMR Spectroscopy. NMR spectra were obtained on a Bruker AMX 500 or 600 spectrometer using standard Bruker software. All measurements were taken on solutions at 27 °C in 0.5 mL of D_2O (pD 6−7) after several lyophilizations with D_2O. Proton spectra were obtained by using a spectral width of 6 kHz and a 90° pulse. The broadband proton-decoupled ^{13}C NMR spectrum was obtained at 125 MHz using a spectral width of 33.3 kHz, a 90° pulse, and WALTZ decoupling (*37*). Acetone was used as the internal standard, and chemical shifts were referenced to the methyl resonance (δ_H, 2.225 ppm; δ_C, 31.07 ppm). Two-dimensional (2D) homonuclear proton correlation (COSY), TOCSY, NOESY, and heteronuclear 2D $^{13}C-^{1}H$ chemical shift correlation (HMQC) experiments were performed as previously described (*28*).

Electrospray Ionization (ESI) Mass Spectrometry. Samples were analyzed on a VG Quattro mass spectrometer (Fisons Instruments) fitted with an electrospray ion source. O-Deacylated LPS and backbone OS samples were dissolved in water which was then mixed in a 1:1 ratio with 50% aqueous acetonitrile containing 0.4% acetic acid for mass spectral analysis in either the negative or positive ion mode. Samples were injected by direct infusion at 4 μL/min with a Harvard syringe pump 22. The electrospray tip voltage was 2.5 kV. The mass spectrometer was scanned from *m*/*z* 150 to 2500 with a scan time of 10 s. Data were collected in multichannel analysis mode, and data processing was handled by the VG data system (Masslynx).

CE-ESI-MS experiments were performed on a API 300 triple-quadrupole mass spectrometer (Perkins Elmer/Sciex) (*38*). A Crystal model 310 CE instrument (ATI Unicam) was coupled to the mass spectrometer via a coaxial sheath-flow interface. A sheath solution of 2-propanol and methanol (70:30) was delivered at a flow rate of 1.5 μL/min to a low dead volume tee (250 μm inside diameter, Chromatographic Specialties Inc.). All aqueous solutions were filtered through a 0.45 μm filter (Millipore) before being used. An electro-

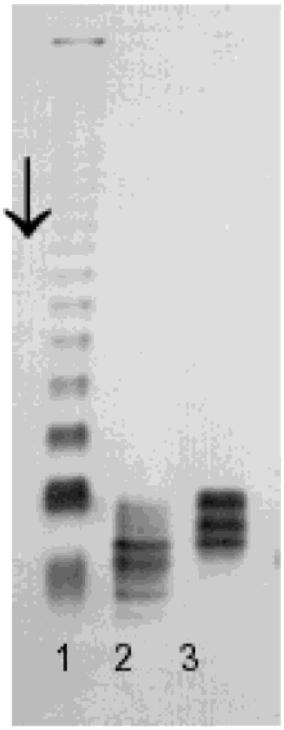

FIGURE 1: DOC−PAGE pattern of LPS from *Salmonella milwaukee* strain and *H. influenzae* type b: lane 1, *S. milwaukee* (S-type LPS, 10 μg); lane 2, *H. influenzae* strain Eagan (4 μg); and lane 3, *H. influenzae* strain RM7004 (4 μg).

spray stainless steel needle (27 gauge) was butted against the low dead volume tee and enabled the delivery of the sheath solution to the end of the capillary column. Separations were obtained on 90 cm (length) bare fused silica using 30 mM aqueous morpholine acetate (pH 9) containing 5% methanol. A voltage of 25 kV was applied at the injection end of the capillary, and spectra were obtained in the negative ion mode. The outlet of the fused-silica capillary (185 μm outside diameter × 50 μm inside diameter) was tapered to an outside diameter of 75 μm (20 μm inside diameter). Data were acquired and processed in the Mass Lynx Windows NT-based data system. The calculation of oligosaccharide molecular masses was facilitated using the computer program "Gretta's carbos" developed by W. Hines (University of California, San Francisco, CA).

RESULTS

Isolation and Characterization of LPS. LPS from *H. influenzae* strain RM7004 was isolated by using the hot phenol−water extraction method (*22*) in a yield of ca. 2−3% from dried bacterial cells. Deoxycholate−polyacrylamide gel electrophoresis (DOC−PAGE) analysis of the LPS indicated that it is a short-chain LPS, consistent with earlier investigations (*7*, *39*). The LPS exhibited a heterogeneous mixture comprised of several bands having electrophoretic mobilities between those of the Ra and SR bands of S-type *Salmonella* LPS (Figure 1, lanes 1 and 3). The electrophoretic mobilities of the major bands were slower than those of the related type b strain, Eagan (Figure 1, lanes 2 and 3), indicating the presence of higher-molecular mass LPS species. We have previously shown that Hex5 comprises the major LPS glycoform population in strain Eagan (*7*). Glycose analysis of the LPS from strain RM7004 indicated the presence of D-glucose (Glc), D-galactose (Gal), L-*glycero*-D-*manno*-heptose (Hep), and 2-amino-2-deoxy-D-glucose (GlcN), which were identified by GLC−MS analysis of the corresponding alditol acetate and 2-butyl glycoside derivatives. Mild acid hydrolysis (1% HOAc, 100 °C, 2 h) of the LPS sample afforded core oligosaccharide and insoluble lipid A fractions. Sugar analysis indicated that GlcN is present only in the lipid A component. The presence of KDO was confirmed by MS and NMR analysis (see below).

O-Deacylated LPS (LPS-OH) was prepared by treatment of the LPS sample with anhydrous hydrazine (37 °C for 1 h). Analysis of LPS-OH samples by electrospray ionization mass spectrometry (ESI-MS) in the negative ion mode revealed a series of related structures that differed in the number of hexose residues (Table 1). It is now well-established that *H. influenzae* LPS is comprised of a conserved inner-core heptose trisaccharide (basal unit) attached to the lipid A moiety via a phosphorylated KDO residue in which the central Hep is substituted with phosphoethanolamine (PEA) (*8*). Under the conditions that were employed, the ESI mass spectra showed peaks corresponding to doubly and triply charged molecular ions (Table 1). The triply charged molecular ions at *m*/*z* 866.0, 920.1, 974.0, 1028.1, 1082.0, and 1136.1, together with the corresponding doubly charged counterparts, indicated the presence of glycoforms containing four to nine hexose residues, respec-

Table 1: Negative Ion ESI-MS Data and Proposed Compositions for O-Deacylated LPS from *H. influenzae* RM7004

	observed ion (*m*/*z*)		molecular mass (Da)		
LPS glycoform	$(M - 3H)^{3-}$	$(M - 2H)^{2-}$	observed[a]	calculated[b]	proposed composition
Hex4	866.0	1299.4	2600.9	2601.3	Hex_4 Hep_3 PEA_1 P_1 KDO_1 lipid A-OH
	906.7	1361.1	2723.7	2724.4	Hex_4 Hep_3 PEA_2 P_1 KDO_1 lipid A-OH
Hex5	920.1	1380.4	2763.1	2763.5	Hex_5 Hep_3 PEA_1 P_1 KDO_1 lipid A-OH
	961.3	1441.5	2886.0	2886.5	Hex_5 Hep_3 PEA_2 P_1 KDO_1 lipid A-OH
Hex6	974.0	1461.8	2925.3	2925.6	Hex_6 Hep_3 PEA_1 P_1 KDO_1 lipid A-OH
	1015.1	1523.0	3048.2	3048.6	Hex_6 Hep_3 PEA_2 P_1 KDO_1 lipid A-OH
Hex7	1028.1	1542.8	3087.5	3087.5	Hex_7 Hep_3 PEA_1 P_1 KDO_1 lipid A-OH
	1068.5	1603.7	3209.0	3210.5	Hex_7 Hep_3 PEA_2 P_1 KDO_1 lipid A-OH
Hex8	1082.0	1623.8	3249.0	3249.7	Hex_8 Hep_3 PEA_1 P_1 KDO_1 lipid A-OH
	1123.0	−	3372.0	3372.7	Hex_8 Hep_3 PEA_2 P_1 KDO_1 lipid A-OH
Hex9	1136.1	−	3411.3	3411.9	Hex_9 Hep_3 PEA_1 P_1 KDO_1 lipid A-OH
	1177.3	−	3534.9	3534.9	Hex_9 Hep_3 PEA_2 P_1 KDO_1 lipid A-OH

[a] Calculated average values of doubly and triply charged ions. [b] Average mass units were used for calculation (*41*) of molecular mass values based on proposed compositions as follows: 162.15 for Hex, 192.17 for Hep, 220.18 for KDO, 79.98 for phosphate, 123.05 for PEA, and 953.03 for lipid A-OH.

Table 2: Negative Ion CE-ESI-MS Data and Proposed Compositions for O-Deacylated LPS from *H. influenzae* RM7004

isomeric LPS glycoform	elution point (min)	molecular mass (Da) observed[a]	molecular mass (Da) calculated[b]	relative distribution (%)	proposed composition
Hex9	10.82	3575.5 (3−)	3574.1	0.5	Hex_9 Hep_3 PEA_2 P_1 KDO_1 lipid A-OH(K^+)[c]
	11.22	3411.0 (3−)	3411.9	0.7	Hex_9 Hep_3 PEA_1 P_1 KDO_1 lipid A-OH
Hex8	11.06	3372.5 (3−)	3372.9	4.5	Hex_8 Hep_3 PEA_2 P_1 KDO_1 lipid A-OH
	11.38	3249.0 (3−)	3249.8	1.6	Hex_8 Hep_3 PEA_1 P_1 KDO_1 lipid A-OH
Hex7	11.22	3210.0 (3−)	3210.7	2.8	Hex_7 Hep_3 PEA_2 P_1 KDO_1 lipid A-OH
	11.62	3087.0 (3−)	3087.7	1.4	Hex_7 Hep_3 PEA_1 P_1 KDO_1 lipid A-OH
Hex6	11.46	3048.5 (3−)	3048.6	5.3	Hex_6 Hep_3 PEA_2 P_1 KDO_1 lipid A-OH
	11.78	2925.0 (2−)	2925.5	2.5	Hex_6 Hep_3 PEA_1 P_1 KDO_1 lipid A-OH
	11.86	2925.0 (3−)	2925.5	5.7	Hex_6 Hep_3 PEA_1 P_1 KDO_1 lipid A-OH
Hex5	11.78	2886.0 (2−)	2886.5	7.6	Hex_5 Hep_3 PEA_2 P_1 KDO_1 lipid A-OH
	11.62	2802.0 (2−)	2802.5	0.6	Hex_5 Hep_3 PEA_1 P_1 KDO_1 lipid A-OH(K^+)
	12.18	2802.0 (2−)	2802.5	0.4	Hex_5 Hep_3 PEA_1 P_1 KDO_1 lipid A-OH(K^+)
	12.18	2762.5 (2−)	2762.4	10.3	Hex_5 Hep_3 PEA_1 P_1 KDO_1 lipid A-OH
Hex4	11.94	2724.0 (2−)	2724.3	1.6	Hex_4 Hep_3 PEA_2 P_1 KDO_1 lipid A-OH
	12.18	2724.0 (2−)	2724.3	1.0	Hex_4 Hep_3 PEA_2 P_1 KDO_1 lipid A-OH
	11.66	2640.0 (2−)	2640.3	0.3	Hex_4 Hep_3 PEA_1 P_1 KDO_1 lipid A-OH(K^+)
	11.94	2640.0 (2−)	2640.3	1.2	Hex_4 Hep_3 PEA_1 P_1 KDO_1 lipid A-OH(K^+)
	12.34	2640.0 (2−)	2640.3	0.3	Hex_4 Hep_3 PEA_1 P_1 KDO_1 lipid A-OH(K^+)
	11.78	2600.5 (2−)	2601.3	0.7	Hex_4 Hep_3 PEA_1 P_1 KDO_1 lipid A-OH
	12.02	2600.5 (2−)	2601.3	0.5	Hex_4 Hep_3 PEA_1 P_1 KDO_1 lipid A-OH
	12.34	2600.5 (2−)	2601.3	6.5	Hex_4 Hep_3 PEA_1 P_1 KDO_1 lipid A-OH
	12.58	2600.5 (2−)	2601.3	1.6	Hex_4 Hep_3 PEA_1 P_1 KDO_1 lipid A-OH
	12.66	2724.0 (2−)	2724.3	0.5	Hex_4 Hep_3 PEA_2 P_1 KDO_1 lipid A-OH
Hex3	12.10	2478.0 (2−)	2478.1	2.8	Hex_3 Hep_3 PEA_1 P_1 KDO_1 lipid A-OH (K^+)
	12.34	2478.0 (2−)	2478.1	2.4	Hex_3 Hep_3 PEA_1 P_1 KDO_1 lipid A-OH (K^+)
	12.26	2438.5 (2−)	2439.1	2.7	Hex_3 Hep_3 PEA_1 P_1 KDO_1 lipid A-OH
	12.82	2438.5 (2−)	2439.1	4.3	Hex_3 Hep_3 PEA_1 P_1 KDO_1 lipid A-OH
	12.42	2562.0 (2−)	2562.2	0.9	Hex_3 Hep_3 PEA_2 P_1 KDO_1 lipid A-OH
Hex2	12.58	2276.5 (2−)	2276.9	0.7	Hex_2 Hep_3 PEA_1 P_1 KDO_1 lipid A-OH
	13.31	2276.5 (2−)	2276.9	0.4	Hex_2 Hep_3 PEA_1 P_1 KDO_1 lipid A-OH
	12.82	2400.0 (2−)	2400.1	0.5	Hex_2 Hep_3 PEA_2 P_1 KDO_1 lipid A-OH
	13.06	2400.0 (2−)	2400.1	0.3	Hex_2 Hep_3 PEA_2 P_1 KDO_1 lipid A-OH
Hex1	13.06	2154.0 (2−)	2153.9	8.1	Hex_1 Hep_3 PEA_1 P_1 KDO_1 lipid A-OH(K^+)
	13.06	2114.0 (2−)	2114.8	0.4	Hex_1 Hep_3 PEA_1 P_1 KDO_1 lipid A-OH
	13.57	2114.0 (2−)	2114.8	0.3	Hex_1 Hep_3 PEA_1 P_1 KDO_1 lipid A-OH
	13.87	2114.0 (2−)	2114.8	2.2	Hex_1 Hep_3 PEA_1 P_1 KDO_1 lipid A-OH
Hex0	13.63	1992.0 (2−)	1991.7	2.7	Hep_3 PEA_1 P_1 KDO_1 lipid A-OH(K^+)
	14.27	1952.5 (2−)	1952.7	0.6	Hep_3 PEA_1 P_1 KDO_1 lipid A-OH
	14.51	1871.5 (2−)	1872.7	0.3	Hep_3 PEA_1 KDO_1 lipid A-OH

[a] Isotope-average molecular mass; most abundant charge state indicated in parentheses. [b] Calculated using molecular mass values given in Table 1. [c] Potassium adduct.

tively, attached to the basal unit (*7*, *33*, *39*−*41*). Similar glycoform compositions of O-deacylated LPS from type b *H. influenzae* strains have been previously reported (*7*, *40*, *42*). Glycoforms containing five and six hexose residues were found to be most abundant from their relative peak intensities. A parallel series of triply and doubly charged ions shifted 123 amu to higher mass could be attributed to glycoform populations that contain an extra PEA. This was especially evident in ESI-MS of the LPS-OH sample when the LPS sample was obtained by ethanol precipitation as observed previously (*7*).

On-line coupling of capillary zone electrophoresis to electrospray mass spectrometry (CE-ESI-MS) was used to separate and characterize the various O-deacylated LPS species (*38*). This technique was particularly useful in establishing the presence of several isomeric glycoforms having the same composition. CE-ESI-MS revealed isomeric LPS-OH glycoforms varying in the number and positions of hexose residues (Table 2). This is shown in Figure 2 for Hex4 glycoforms in which four isomeric forms having a Hex_4 Hep_3 PEA_1 P_1 KDO_1 lipid A-OH composition eluted between 11.78 and 12.58 min. The most prominent glycoform (representing 70% of the four isomeric forms) observed at 12.34 min was subsequently shown to carry hexose substituents on each of the heptoses in the triheptosyl inner-core unit with a disaccharide on the central heptose being substituted with a disaccharide. The structures of the major isomeric glycoforms that contained four to nine hexose residues were determined by NMR spectroscopy (see below).

Characterization of LPS Backbone Oligosaccharides. Oligosaccharides, representative of intact LPS glycoforms, were obtained following complete deacylation (hydrazine treatment), dephosphorylation (aqueous HF), and reduction ($NaBH_4$) of the terminal glucosamine unit (*27*). Oligosaccharides obtained in this way were fractionated using size exclusion gel filtration chromatography on Bio-Gel P2. Three major OS fractions were obtained following repetitive (three times) chromatographic fractionation (Fr.1−Fr.3). Positive ion ESI-MS of the fractions revealed a series of related oligosaccharides containing between three and nine hexose residues (Table 3). Methylation analysis data for the OS fractions are presented in Table 4. Each of the three fractions contained the same methylated components but in differing relative proportions. The 3,4-di-O-substituted Hep*p*, 2,3-di-O-substituted Hep*p*, 2-O-substituted Hep*p*, 4-O-substituted Glc*p*, 4-O-substituted Gal*p*, and terminal Glc*p*, Gal*p*, and

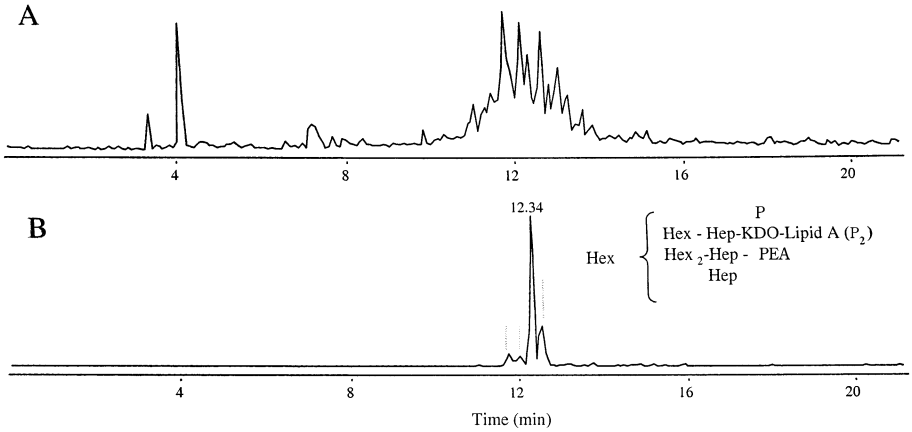

FIGURE 2: Negative ion CE-ESI-MS of O-deacylated LPS from *H. influenzae* strain RM7004. (A) Total ion electropherogram (*m*/*z* 300−1500) showing separation of isomeric glycoforms. (B) Selective ion monitoring at *m*/*z* 1299 for doubly charged ions from Hex4 glycoforms. A structural model for isomeric Hex4 glycoforms is shown in the inset. Major Hex4 glycoform populations carry a galactose residue off the distal heptose of the basal unit.

Table 3: Positive Ion ESI-MS Data and Proposed Compositions for LPS Backbone Oligosaccharide Fractions Derived from *H. influenzae* Strain RM7004[a]

OS glycoform	observed ion (*m*/*z*) $[(M + 2H)^{2+}]$	molecular mass (Da) observed	calculated[b]	proposed composition
Hex3	813.0	1624.0	1623.4	Hex_3 Hep_3 KDO_1 $HexN_2$
Hex4	894.5	1787.0	1785.6	Hex_4 Hep_3 KDO_1 $HexN_2$
Hex5	975.8	1949.6	1947.8	Hex_5 Hep_3 KDO_1 $HexN_2$
Hex6	1056.8	2111.6	2109.9	Hex_6 Hep_3 KDO_1 $HexN_2$
Hex7	1137.5	2273.0	2272.0	Hex_7 Hep_3 KDO_1 $HexN_2$
Hex8	1218.7	2435.4	2434.2	Hex_8 Hep_3 KDO_1 $HexN_2$
Hex9	1300.0	2598.0	2596.3	Hex_9 Hep_3 KDO_1 $HexN_2$

[a] Data obtained from Fr.1 containing a mixture of Hex6−Hex9 glycoforms with Hex7 and Hex8 as the major forms, from Fr.2 containing Hex5 and Hex6 glycoforms, and from Fr.3 containing Hex3−Hex5 glycoforms with Hex4 and Hex5 as the major forms. [b] Average mass units were used for calculation (*41*) of molecular mass values based on the proposed composition as follows: 162.15 Da for Hex, 192.17 Da for Hep, 220.18 Da for KDO, and 161.15 Da for HexN.

Table 4: Methylation Analysis of the LPS Backbone OS Fractions Derived from *H. influenzae* Strain RM7004

methylated sugar[a] (as alditol acetate)	T_m[b]	relative detector response[c] Fr.1	Fr.2	Fr.3	substitution pattern
2,3,4,6-Me_4-D-Glc	1.00	0.06	0.11	0.23	D-Glc*p*-(1→
2,3,4,6-Me_4-D-Gal	1.07	1.00	1.00	1.00	D-Gal*p*-(1→
2,3,6-Me_3-D-Gal	1.34	0.68	0.37	0.15	→4)-D-Gal*p*-(1→
2,3,6-Me_3-D-Glc	1.35	1.36	0.98	1.00	→4)-D-Glc*p*-(1→
2,3,4,6,7-Me_5-LD-Hep	1.54	0.13	0.08	0.08	LD-Hep*p*-(1→
3,4,6,7-Me_4-LD-Hep	1.95	0.14	0.24	0.28	→2)-LD-Hep*p*-(1→
2,6,7-Me_3-LD-Hep	2.36	0.15	0.15	0.16	→3,4)-LD-Hep*p*-(1→
4,6,7-Me_3-LD-Hep	2.53	0.15	0.15	0.17	→2,3)-LD-Hep*p*-(1→

[a] 2,3,4,6-Me_4-D-Glc represents 1,5-di-*O*-acetyl-2,3,4,6-tetra-*O*-methyl-D-glucitol-d_1 and so on. Data for only neutral sugars are reported. Partially methylated glycose derivatives from the GlcN(1→6)GlcN reducing end moiety were not detected, probably due to the relative resistance of the GlcN glycosidic linkage to the conditions used for acid hydrolysis (see Experimental Procedures). [b] Retention times (T_m) are quoted relative to that of 2,3,4,6-Me_4-D-Glc. [c] Values are not corrected for differences in detector response factors and are presented relative to that of 2,3,4,6-Me_4-D-Gal.

Hep*p* residues were identified. Significant amounts of 2,3,4,6-tetra-*O*-methyl-Gal*p* were observed in each of the fractions, indicating a preponderance of oligosaccharide chains capped by a Gal residue at the nonreducing end. The higher-molecular mass fraction (Fr.1) showed a relatively large amount of 2,3,6-tri-*O*-methyl-Gal*p* than the lower-molecular mass fraction (Fr.3). The occurrence of 2,3,4,6,7-penta-*O*-methyl-Hep*p* indicated the presence of glycoforms containing unsubstituted heptose in the inner core (*7*). This was more prevalent in the higher-molecular mass fractions. Comparative analysis of the methylated sugar derivatives showed smaller amounts of 2,6,7-tri-*O*-methyl-Hep*p* and 4,6,7-tri-*O*-methyl-Hep*p* than expected, which could be due to incomplete hydrolysis of resistant Hep−Hep bonds under the relatively mild acid hydrolysis conditions that were employed. By using stronger acidic conditions and longer hydrolysis times, these resistant Hep−Hep bonds in methylated glycoforms have been reported to be hydrolyzed in other *H. influenzae* strains (*6*, *43*).

The structures of the oligosaccharides that were present in each of the three fractions were elucidated by detailed ^{1}H and ^{13}C NMR analysis. The ^{1}H NMR resonances were fully assigned by COSY and TOCSY experiments. Subspectra corresponding to all the glycosyl residues were identified on the basis of the connectivity pathways delineated in the homonuclear chemical shift correlation maps (*7*, *27*, *28*), the chemical shift values (*44*), and the vicinal proton coupling constants (*45*). Assignment of carbon resonances was made by direct correlation of the ^{1}H resonances to the ^{13}C resonances of the directly attached protons in an HMQC experiment, and by comparison of the ^{13}C resonances with the recorded chemical shift data of similar substituted glycosyl residues (*7*, *46*, *47*). The ^{1}H and ^{13}C data are recorded in Tables 5 and 6.

Structure of the Major Hex5 and Hex6 Backbone Oligosaccharides. Fr.2 was the most abundant and homogeneous oligosaccharide fraction. ESI-MS of this fraction showed two molecular ions at *m*/*z* 1056.8 $[(M + 2H)^{2+}]$ and 975.8 $[(M + 2H)^{2+}]$ in the positive ion mode (Table 3), corresponding to Hex6 (M_r = 2111.6 Da) and Hex5 (M_r = 1949.6 Da) glycoforms, respectively (*7*). Significant overlap of resonances was observed in the low-field region (4.7−4.3 ppm) of the one-dimensional (1D) ^{1}H NMR spectrum (Figure 3). Separation of the overlapping signals was achieved in the 2D COSY spectrum (Figure 4A). Nine major anomeric ^{1}H resonances were observed in the low-field region of the spectrum at 5.55 (d, $J_{1,2} \approx 1.0$ Hz), 5.35 (d, $J_{1,2} = 4.1$ Hz), 5.12 (d, $J_{1,2} \approx 1.0$ Hz), 5.09 (d, $J_{1,2} \approx 1.0$ Hz), 4.95 (d, $J_{1,2}$

Table 5: Proton Chemical Shifts (parts per million) and Coupling Constants (hertz) of the Major LPS Backbone Oligosaccharide Glycoforms Derived from *H. influenzae* Strain RM7004[a]

LPS backbone unit[b]	residue	glycose unit	H-1 ($J_{1,2}$)	H-2 ($J_{2,3}$)	H-3 ($J_{3,4}$)	H-4 ($J_{4,5}$)	H-5	H-6 ($J_{5,6}$)	H-6′ ($J_{5,6'}$, $J_{6,6'}$)	H-7 ($J_{6,7}$)	H-7′ ($J_{6,7'}$, $J_{7,7'}$)	H-8 ($J_{7,8}$)	H-8′ ($J_{7,8'}$, $J_{8,8'}$)
Hex5	GlcN*ol*	→6)-D-GlcN*ol*	3.89[c] (4.4)	3.53 (4.6)	4.11 (∼1.0)	3.66 (9.2)	3.96	4.15 (3.5)	3.81 (7.4, 10.4)				
	GlcN	→6)-*β*-D-Glc*p*N-(1→	4.62	2.90	3.61	3.50	3.62	3.59					
	KDO	→5)-α-KDO*p*-(2→			1.85[d] (11.7)	4.18 (5.8)	4.11	3.71		3.78		3.95 (3.5)	3.65 (6.9, 11.5)
	HepI	→3,4)-L-α-D-Hep*p*-(1→	5.09 (1.0)	4.16 (4.6)	4.06 (9.2)	4.26 (10.4)	4.17	4.11 (1.0)		3.72 (∼1.0)	3.72 (∼1.0, 10.4)		
	HepII	→2,3)-L-α-D-Hep*p*-(1→	5.55 (1.0)	4.27 (4.6)	4.10 (9.2)	4.15 (10.4)	3.68	4.08 (∼1.0)		3.62 (5.8)	3.73 (8.1, 10.4)		
	HepIII	→2)-L-α-D-Hep*p*-(1→	5.12 (1.0)	4.06 (4.6)	3.93 (9.2)	3.84 (10.4)	3.81	4.05 (∼1.0)		3.73 (3.5)	3.69 (9.2, 10.4)		
	GlcII	→4)-α-D-Glc*p*-(1→	5.35 (4.1)	3.62 (9.2)	3.85 (9.2)	3.70 (9.2)	3.90	3.96	3.90				
	GlcIII	→4)-*β* -D-Glc*p*-(1→	4.56 (7.5)	4.56 (10.0)	3.68	3.66	3.66	3.99 (3.4)	3.83				
	GalI	*β*-D-Gal*p*-(1→	4.35 (8.1)	3.57 (9.2)	3.67 (4.1)	3.92 (1.0)	3.69	3.75 (4.6)	3.82 (8.1, 11.5)				
	GlcI	*β*-D-Glc*p*-(1→	4.53 (7.5)	3.35 (9.2)	3.46 (9.2)	3.37 (9.2)	3.45	3.95 (1.0)	3.77 (6.9, 11.5)				
	GalII	*β*-D-Gal*p*-(1→	4.45 (8.1)	3.55 (9.2)	3.66 (4.1)	3.92 (∼1.0)	3.72	3.78					
Hex6	GalII*	→4)-*β*-D-Gal*p*-(1→	4.51 (8.8)	3.58 (10.0)	3.74 (3.8)	4.04 (1.0)	3.79	–	–				
	GalIII	α-D-Gal*p*-(1→	4.95 (4.5)	3.84 (10.0)	3.90 (4.5)	4.03 (∼1.0)	4.35	3.72 (6.3)	3.69 (6.3, 11.3)				
Hex7−Hex9[e]	GlcI*	→4)-*β*-D-Glc*p*-(1→	4.58 (8.6)	3.46 (8.6)	3.62 (10.0)	3.50 (8.6)	–	–	–				
	GlcIV*	→4)-*β*-D-Glc*p*-(1→	4.48 (8.6)	3.36 (8.6)	3.65	3.70	–	–	–				
Hex4′−Hex8′	HepI*	→3,4)-L-α-D-Hep*p*-(1→	5.09 (1.0)	4.15 (4.3)	4.08 (10.0)	4.30	4.17	4.05 (1.0)		3.70	3.70		
	HepII*	→2,3)-L-α-D-Hep*p*-(1→	5.71 (1.0)	4.28 (4.3)	4.06 (10.0)	4.12 (10.0)	3.67	4.09 (1.0)		3.63 (5.7)	3.73 (8.6, 11.4)		
	HepIII*	L-α-D-Hep*p*-(1→	5.12 (1.0)	3.83	–	–	–	–					
	GlcII*	→4)-α-D-Glc*p*-(1→	5.30 (4.3)	3.62 (10.0)	3.89 (8.6)	3.73 (10.0)	3.91	3.98 (1.0)	3.83 (5.7, 11.4)				

[a] Measured at 27 °C in D_2O (pD 6) from COSY and TOCSY spectra. [b] Chemical shift values for conserved residues (i.e., residues GlcN*ol*−GalI) in Hex5−Hex9 glycoforms are the same (±0.01 ppm). Hex5 and Hex6 carry GlcI as a terminal group from HepI; Hex5 carries the GalII-GlcIII-GlcII trisaccharide from HepII, while Hex6 carries the GalIII-GalII*-GlcIII-GlcII tetrasaccharide. In the Hex7−Hex9 glycoforms, further chain extension occurs from HepI: a GlcIV-GlcI* disaccharide in Hex7, a GalIV-GlcIV*-GlcI* trisaccharide in Hex8, and a GalV-GalIV*-GlcIV*-GlcI* tetrasaccharide in Hex9. An isomeric population of glycoforms, Hex4′−Hex8′, lacks the GalI residue at HepIII and shows chemical shift differences in the inner core (i.e., HepI*, HepII*, HepIII*, and GlcII*). [c] Values for H-1 and $J_{1,2}$: H-1′ = 3.77 ppm, $J_{1',2}$ = 6.9 Hz, and $J_{1,1'}$ = 12.7 Hz. [d] Values for H-3a and $J_{3a,4}$: H-3e = 2.17 ppm, $J_{3e,4}$ = 3.9 Hz, and $J_{3e,3a} \approx 11.7$ Hz (a and e correspond to the axial and equatorial protons of KDO, respectively). [e] The chemical shifts and coupling constants for GalIV, GalIV*, and GalV residues in the Hex8 and Hex9 glycoforms are indistinguishable from those of GalII, GalII*, and GalIII, respectively. The chemical shifts for GlcIV in Hex7 were not assigned.

Table 6: ^{13}C Chemical Shifts (parts per million) of the Major LPS Backbone Oligosaccharide Glycoforms Derived from *H. influenzae* Strain RM7004[a]

LPS backbone unit[b]	residue	glycose unit	C-1	C-2	C-3	C-4	C-5	C-6	C-7	C-8
Hex5	GlcN*ol*	→6)-*β*-D-GlcN*ol*	59.8	56.3	66.9	72.0	70.3	73.0		
	GlcN	→6)-*β*-D-Glc*p*N-(1→	102.4	57.0	–	71.1	74.7	62.8		
	KDO	→5)-α-KDO*p*-(2→			35.8	66.9	75.5	72.7	70.3	64.5
	HepI	→3,4)-L-α-D-Hep*p*-(1→	101.9	71.1	74.7	74.2	72.5	69.2	64.4	
	HepII	→2,3)-L-α-D-Hep*p*-(1→	100.0	79.8	79.3	66.7	72.6	69.2	64.1	
	HepIII	→2)-L-α-D-Hep*p*-(1→	101.2	78.9	70.8	67.7	72.9	69.6	64.4	
	GlcII	→4)-α-D-Glc*p*-(1→	101.2	72.6	72.5	79.3	72.2	–		
	GlcIII	→4)-*β*-D-Glc*p*-(1→	103.2	73.9	75.5	79.2	75.8	–		
	GalI	*β*-D-Gal*p*-(1→	103.5	71.9	73.5	69.7	76.2	–		
	GlcI	*β*-D-Glc*p*-(1→	103.5	74.5	77.2	71.1	77.2	62.2		
	GalII	*β*-D-Gal*p*-(1→	103.9	71.9	73.5	69.7	76.2	–		
Hex6	GalII*	→4)-*β*-D-Gal*p*-(1→	104.3	71.9	73.0	78.4	76.5	–		
	GalIII	α-D-Gal*p*-(1→	101.3	69.7	70.0	69.9	71.9	61.5		
Hex7−Hex9	GlcI*	→4)-*β*-D-Glc*p*-(1→	103.5	74.2	75.9	–	76.0	–		
	GlcIV*	→4)-*β*-D-Glc*p*-(1→	103.7	74.0	75.2	–	–	–		
Hex4′−Hex8′	HepI*	→3,4)-L-α-D-Hep*p*-(1→	101.8	71.2	74.0	74.0	–	–	–	
	HepII*	→2,3)-L-α-D-Hep*p*-(1→	99.5	80.0	79.8	66.6	–	–	–	
	HepIII*	L-α-D-Hep*p*-(1→	102.8	71.9	–	–	–	–	–	
	GlcII*	→4)-α-D-Glc*p*-(1→	101.2	72.5	72.2	79.0	72.2	60.9		

[a] Measured at 27 °C in D_2O (pD 6) from HMQC spectra. [b] Designations of backbone glycoforms are as in Table 5. Chemical shifts of conserved inner-core residues (GlcNol−GalI in Hex5−Hex9 glycoforms and HepI*−GlcII* in Hex4′−Hex8′ glycoforms) are the same within ±0.1 ppm.

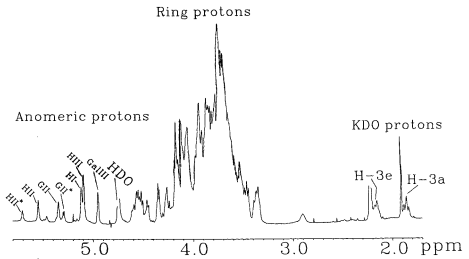

FIGURE 3: ^{1}H spectrum of the LPS backbone oligosaccharide fraction, Fr.2, consisting of major Hex6 and minor Hex5 glycoforms from *H. influenzae* RM7004 recorded in D_2O at pD 6 and 27 °C. The anomeric, ring, and methyl resonances are indicated. Abbreviations are given in the legend of Figure 4. Anomeric ^{1}H assignments marked with an asterisk are from the isomeric Hex5 glycoform, Hex5′.

= 4.5 Hz), 4.56 (d, $J_{1,2}$ = 7.5 Hz), 4.53 (d, $J_{1,2}$ = 7.5 Hz), 4.45 (d, $J_{1,2}$ = 8.1 Hz), and 4.35 ppm (d, $J_{1,2}$ = 8.1 Hz), and four minor anomeric ^{1}H resonances at 5.71 (d, $J_{1,2} \approx 1.0$ Hz), 5.30 (d, $J_{1,2}$ = 4.3 Hz), 5.12 (d, $J_{1,2} \approx 1.0$ Hz), and 5.09 ppm (d, $J_{1,2} \approx 1.0$ Hz) were also observed (Table 5 and Figures 4A and 5A). The minor resonances could be attributed to oligosaccharide components in the sample that were lacking one sugar residue from HepIII in the basal unit (GalI; see below). In addition, diagnostic signals from the equatorial and axial H-3 methylene protons from a single α-linked KDO pyranosyl residue were identified at 2.17 ($J_{3e,4}$ = 3.9 Hz, $J_{3e,3a}$ = 11.7 Hz) and 1.85 ppm ($J_{3e,3a}$ = 11.7 Hz), respectively (*7*, *27*, *28*, *48*−*50*). The ^{13}C NMR signal in the high-field region of the spectrum from the methylene carbon (C-3) of the KDO was observed at 35.8 ppm (*7*, *27*, *28*). The 2D ^{1}H−^{13}C correlation map was particularly valuable for identifying resonances in the *β*-anomeric region of the spectra (Figure 5A).

The anomeric resonances served as the starting point for 2D spectral analysis, from which subspectra corresponding to the ring systems for each of the glycosyl residues were identified in COSY (Figure 4A) and TOCSY (data not shown) spectra. The three heptose residues (HepI−HepIII) were assigned on the basis of the observed small $J_{1,2}$ (∼1 Hz) and $J_{2,3}$ (4.6 Hz) values, which pointed to *manno*-

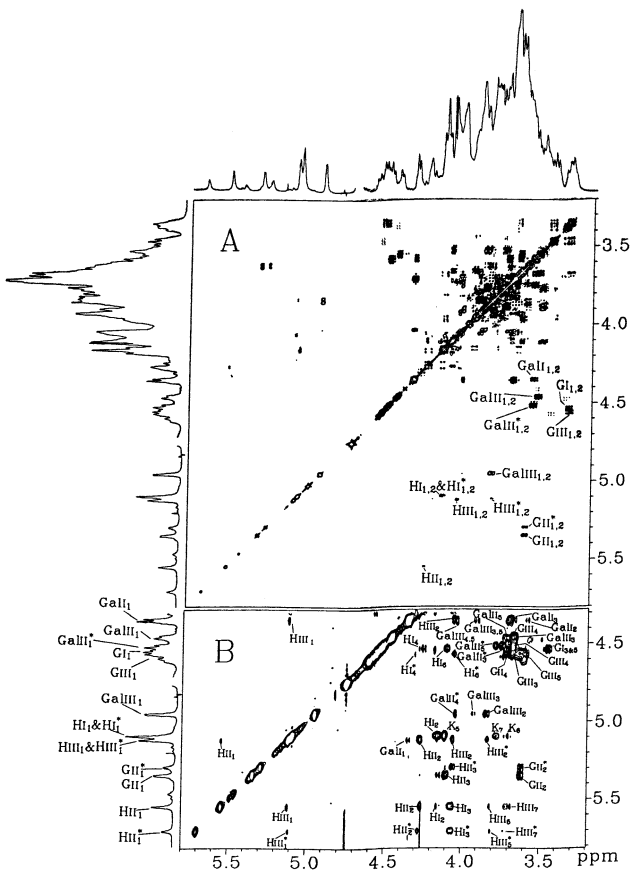

FIGURE 4: Partial 2D COSY (A) and NOESY (B) spectra of LPS backbone OS fraction, Fr.2, from *H. influenzae* RM7004. Cross-peaks relating anomeric and H-2 protons and NOE connectivities are shown in spectra A and B, respectively. Cross-peaks labeled with an asterisk are from isomeric Hex5 backbone oligosaccharides due to the absence of GalI or GalIII. Cross-peaks relating H-1 and H-2 of the minor residue HII* were weak in the COSY spectrum and are not visible at the indicated contour level. Abbreviations: HepI−HepIII, HI−HIII; GlcI−GlcIII, GI−GIII; KDO, K.

pyranosyl ring systems, and by the fact that eight ^{1}H and seven ^{13}C resonances could be associated with each subspectrum. The anomeric ^{1}H and ^{13}C chemical shift values

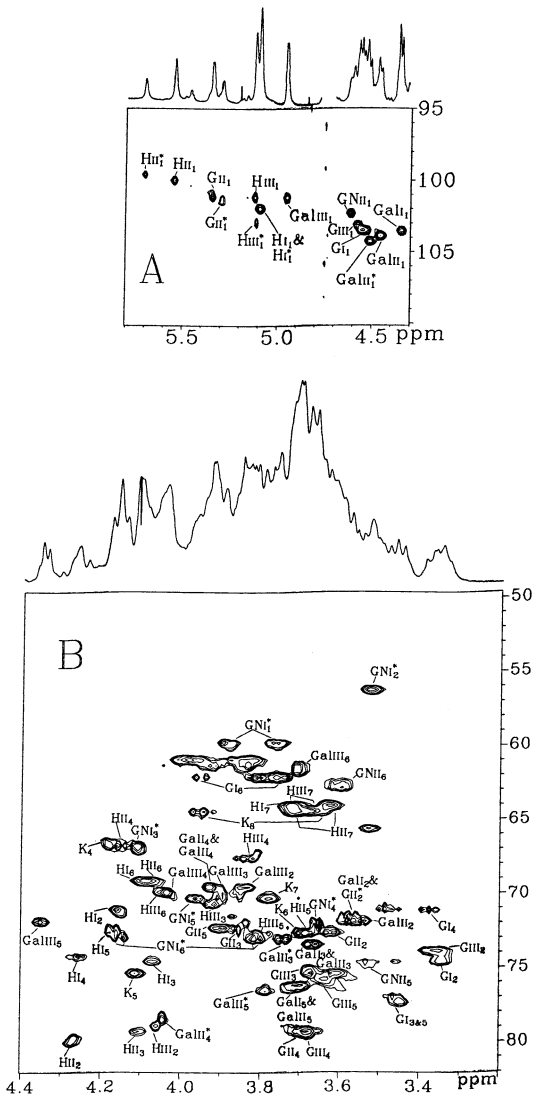

FIGURE 5: Heteronuclear 2D $^{13}C-^{1}H$ chemical shift correlation map of (A) the anomeric and (B) ring regions of the backbone OS fraction, Fr.2, from *H. influenzae* RM7004. Assignments are indicated, and the abbreviations are given in the legend of Figure 4.

(*7*, *27*) indicated that each of the heptose residue has the α-D configuration, and this was confirmed by the occurrence of a single intraresidue NOE between H-1 and H-2 resonances (*51*).

On the basis of the large magnitude of the vicinal couplings $J_{2,3}$, $J_{3,4}$, and $J_{4,5}$ (9−10 Hz), two ^{1}H subspectra having the *gluco* configuration were readily identified (labeled GlcI and GlcII). One of them (GlcI, 4.53 ppm) was shown to have the β configuration ($J_{1,2} = 7.5$ Hz), and the other residue (GlcII, 5.35 ppm) was shown to have the α configuration ($J_{1,2} = 4.1$ Hz). Analogously, two ^{1}H subspectra were attributed to β-linked *galacto*-pyranosyl units (GalI and GalII) based on their observed vicinal coupling of $J_{1,2}$, $J_{2,3}$, $J_{3,4}$, and $J_{4,5}$ (8.1, 9.1, 4.1, and ∼1.0 Hz, respectively), while one ^{1}H subspectrum (GalIII, 4.95 ppm) was identified as an α-linked *galacto*-pyranosyl unit ($J_{1,2} = 4.5$ Hz, $J_{2,3} = 10.0$ Hz, $J_{3,4} = 4.5$ Hz, and $J_{4,5} \sim 1.0$ Hz). The magnitude of the vicinal couplings for another ^{1}H subspectrum was not well-resolved in the COSY spectrum but could be attributed to a *gluco*-pyranosyl residue (GlcIII) on the basis of a comparison of chemical shift data with that of strain Eagan

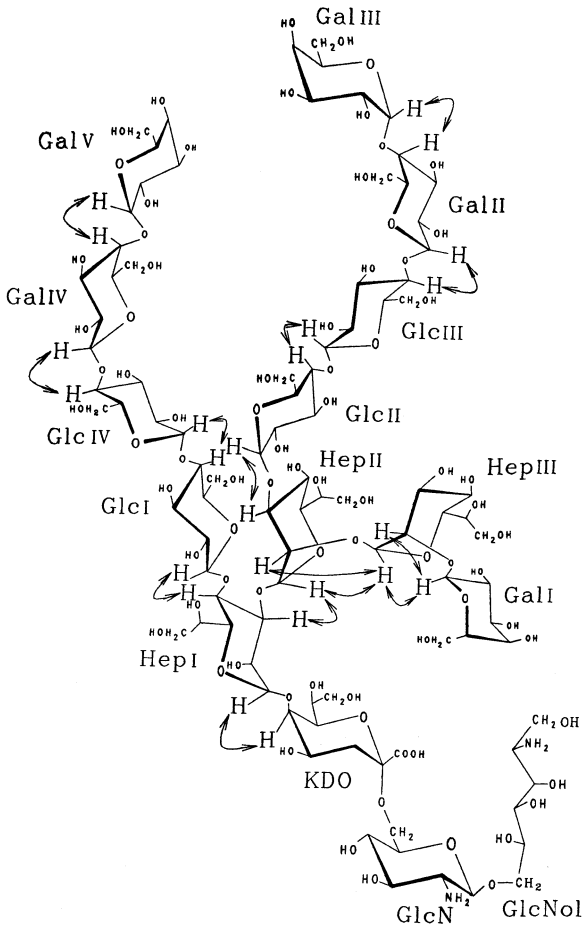

FIGURE 6: Structure of the Hex9 backbone OS from *H. influenzae* RM7004 illustrating the connectivity network of observed transglycosidic NOE connectivities.

(*7*). From the magnitude of the $J_{1,2}$ couplings, a β-D configuration was assigned to GlcIII ($J_{1,2} = 7.5$ Hz). The high-field methylene proton resonances (H-3's) of KDO served as the starting point in identifying the subspectrum corresponding to the KDO ring system by COSY analysis (Table 5).

Two characteristic ^{13}C resonances at 56.3 and 57.0 ppm were observed in the HMQC spectrum, which were attributed to amino-substituted sugar residues (*46*) assigned to the glucosamine disaccharide component of the lipid A moiety of the LPS (*33*, *52*). The ^{13}C resonance at 57.0 ppm correlated to the H-2 resonance (2.90 ppm) from the ^{1}H spin system of the β-D-glucosamine (GlcNII), while the ^{13}C resonance at 56.3 ppm correlated to the H-2 resonance (3.53 ppm) of the glucosamintol end group (GlcN*ol*) (*7*, *27*, *28*). A cross-peak observed in the anomeric region ($\delta_H = 4.62$ ppm, $\delta_c = 102.4$ ppm) in the HMQC spectrum (Figure 5A) could be assigned to the β-glucosamine residue (GlcNII).

The chemical shift data for the major glycose ring systems in Fr.2 were closely correlated with those of the Hex6 backbone oligosaccharide observed as a minor glycoform in *H. influenzae* strain Eagan (*7*). The structural identity of the glycoforms was confirmed by NOE experiments. Transglycosidic proton NOE connectivities between anomeric and aglyconic protons on adjacent glycosidically linked residues were measured in the two-dimensional mode. Part of the NOESY contour plot is shown in Figure 4B, and connectivities are shown in Figure 6. Intense transglycosidic NOEs

were observed between HepIII H-1 and HepII H-2, HepII H-1 and HepI H-3, HepI H-1 and KDO H-5 resonances, which established the linear sequence of the triheptosyl region of the backbone OS as L-α-D-Hep*p*-(1→2)-L-α-D-Hep*p*-(1→3)-L-α-D-Hep*p*-(1→5)-α-KDO*p*.

The NOE data indicate that the HepI and HepII residues are further substituted with hexose extensions. The occurrence of transglycosidic NOEs between GlcI H-1 and HepI H-4/H-6 and between GlcII H-1 and HepII H-3 were indicative of substitution at O-4 of HepI and at O-3 of HepII with the β- and α-D-glucose residues, respectively. The ^{13}C chemical shift value of the C-4 resonance for the O-4-substituted heptose (HepI) showed a significant downfield shift of ≈7 ppm compared to those of analogous residues not substituted at that position (e.g., HepII and HepIII) (Table 6). A similar pattern of NOE connectivities was previously observed (*7*). The presence of the globoside trisaccharide, α-D-Gal*p*-(1→4)-β-D-Gal*p*-(1→4)-β-D-Glc*p*-(1→, was established from the observed transglycosidic NOE connectivities between GalIII H-1 and GalII* H-4 and between GalII* H-1 and GlcIII H-3 and/or H-4. The occurrence of a strong NOE between H-1 of the α-D-Gal*p* residue (GalIII) and only H-4 of the β-D-Gal*p* residue (GalII*) clearly established the 1,4-linkage of the terminal galabiose unit, and this was confirmed from the methylation analysis data (Table 4). It is noteworthy that strong NOE connectivities are generally observed between H-1 and H-4 as well as between H-1 and H-3 in 1,3-linked α-D-Gal*p*-β-D-Gal*p* disaccharide units (*53*). The trisaccharide side chain was attached to the α-Glc*p* off HepII as evidenced by a NOE connectivity between GlcIII H-1 and GlcII H-4. Methylation analysis was consistent with substitution at O-4 of the two Glc residues (GlcII and GlcIII) (Table 4). The ^{13}C chemical shift data indicated that the ^{13}C resonances at the substituted sites of the glycosyl residues showed significant downfield shifts compared to those of unsubstituted analogous glycosyl residues, in accord with the assigned positions of substitution deduced from NOE connectivities. Thus, as expected, the ^{13}C resonance of GlcIII C-4 showed a significant downfield shift of 8.1 ppm with the concomitant upfield shift (1.7 ppm) for the adjacent C-3, compared to unsubstituted β-D-glucose (GlcI) (Table 6).

HepIII is partially substituted at the O-2 position by GalI, the occurrence of substitution being determined from the observed transglycosidic NOE between GalI H-1 and HepIII H-2. Transglycosidic NOEs were also observed between GalI H-1 and HepIII H-1 and between HepII H-1 and HepIII H-1 (Figure 4B), an indication of the proximity (<3 Å) of the anomeric protons of GalI, HepIII, and HepII residues in these glycoforms. The partial substitution of HepIII with β-D-Gal*p* is responsible for the observed heterogeneity in the NMR spectra of backbone OS in Fr.2. The absence of GalI from the backbone OS caused chemical shift differences for ^{1}H and ^{13}C resonances on adjacent glycosyl residues (Figures 4 and 5, labeled HI*, HII*, HIII*, and GII*), indicating the presence of an isomeric series of glycoforms in which HepIII is unsubstitued. This is consistent with the methylation analysis results (Table 4), where a derivative corresponding to a terminal heptose was observed. Parts of the ^{1}H spin systems corresponding to HepI*, HepII*, terminal HepIII*, and GlcII* were identified from COSY and TOCSY experiments (Table 5), and the corresponding ^{13}C resonances were identified from the HMQC spectrum (Table 6). The linkage positions of the glycosyl residues in the lipid A backbone region were deduced from the previously determined structure of the deep-rough chemotype of *H. influenzae* strain I-69 Rd^{-}/b^{+} (*33*, *52*), which showed that the lipid A backbone is composed of β-(1′,6)-linked glucosamine disaccharide substituted with KDO at the O-6′ position of the nonreducing glucosamine.

Structural Identification of Extended Oligosaccharides in Fr.1. ESI-MS of Fr.1 showed molecular ions at *m*/*z* 1137.5 [$(M + 2H)^{2+}$], 1218.7 [$(M + 2H)^{2+}$], and 1300.0 [$(M + 2H)^{2+}$], corresponding to OS glycoforms containing seven (M_r = 2273.0 Da), eight (M_r = 2435.4 Da), and nine (M_r = 2598.0 Da) hexose residues, respectively (Table 3). The detailed structures of the OS components from Fr.1 were elucidated by 2D NMR spectroscopy. Two additional ^{1}H spin systems were identified in the backbone OS, indicating the presence of extended glycoforms from HepI (GlcI* and GlcIV*) (Table 5). In addition, intense cross-peak signals in the COSY spectrum were observed for the ^{1}H spin systems from residues GalII* and GalIII, pointing to the presence of spin systems from two similar overlapping residues. This was evident from the NOESY experiment in which transglycosidic NOEs were observed between GalIII H-1 and GalII* H-4, GalII* H-1 and GlcIV* H-4, GlcIV* H-1 and GlcI* H-4, and GlcI* H-1 and HepI H-4/H-6 resonances, establishing the sequence of the fully extended side chain extension on the HepI as α-D-Gal*p*-(1→4)-β-D-Gal*p*-(1→4)-β-D-Glc*p*-(1→4)-β-D-Glc*p*-(1→4)-L-α-D-Hep*p* (Figure 6). In addition, NOEs were observed between GalII* H-1 and GlcIII H-4, clearly indicating the presence of two tetrasaccharide units in the Hex9 glycoform. For the extension on HepI, the terminal galabiose unit was labeled GalV−GalIV* where GalII* and GalIV*, and GalIII and GalV, have identical spin-systems. The occurrence of the isomeric series of glycoforms in which HepIII is unsubstituted was found to be particularly prominent in Fr.1 as evidenced by the relative ratio of the anomeric signals from HepII and HepII* which indicated only 30% substitution at HepIII. The backbone structures of Hex9 (and Hex8′) OS glycoforms containing two tetrasaccharide side chains from the branching HepI and HepII residues are shown in Figure 7. Methylation analysis of Fr.1 showed a relative increase in 4-O-substituted Glc and Gal derivatives, and a concomitant decrease in the relative ratio of the terminal Glc (GlcI) compared to Fr.2 (Table 4), which also pointed to the presence of two extended OS chains from HepI and HepII of the inner core in Hex7−Hex9 glycoform populations.

Structural Identification of More Truncated Oligosaccharides in Fr.3. The structures of the oligosaccharides in Fr.3 were found to be similar to that of the major Hex6 glycoform but lacking one or two galactose residues (GalIII and GalII) from the tetrasaccharide side chain off HepII. ESI-MS analysis of Fr.3 showed two major molecular ions at *m*/*z* 975.0 [$(M + 2H)^{2+}$] and 894.5 [$(M + 2H)^{2+}$], in addition to a minor peak at 813.0 [$(M + 2H)^{2+}$] corresponding to glycoforms containing five (M_r = 1949.6 Da), four (M_r = 1787.0 Da), and three (M_r = 1624.0 Da) hexose residues, respectively (Table 3). The truncated trisaccharide side chain was concluded from the occurrence of a major ^{1}H spin system corresponding to the terminal β-D-Gal*p* residue (GalII) in Fr.3 (Table 5). Correspondingly, ^{13}C NMR

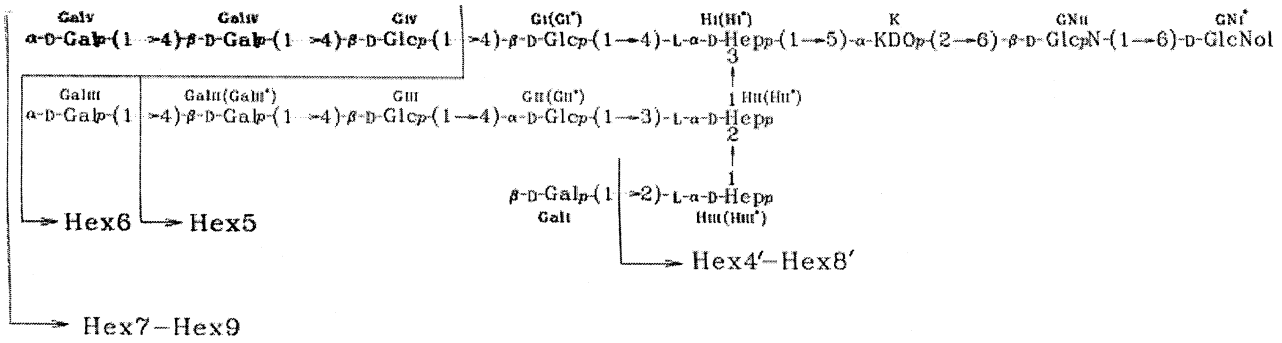

FIGURE 7: Structural model of *H. influenzae* RM7004 LPS showing the major isomeric glycoforms. Isomeric glycoforms lacking the β-D-Gal*p* residue (GalI) on the distal heptose are labeled with a prime′.

chemical shifts determined from the HMQC spectrum for this residue were in accord with those reported (*7*) for terminal β-D-Gal*p* residues (Table 5). In addition, a minor ^{1}H spin system corresponding to a terminal β-D-Glc*p* residue (GlcIII) in Fr.3 was also observed (data not shown), pointing to the presence of minor OS glycoform populations that carry a cellobiose unit (GlcII and GlcIII) on central heptose (HepII). This was supported by the observed reduction in the relative proportion of 2,3,6-tri-*O*-methyl-D-galactopyranose and the concomitant increase in the proportion of 2,3,4,6-tetra-*O*-methyl-D-glucopyranose in methylation analysis of Fr.3 compared to Fr.2 (Table 4). Moreover, the presence of 3,4,6,7-tetra-*O*-methyl-D-heptopyranose and 2,3,4,6,7-penta-*O*-methyl-D-heptopyranose derivatives due to partial substitution of HepIII (Table 4) is consistent with the observed heterogeneity.

Structure of LPS Glycoforms. Phosphate substitution in LPS glycoforms was found to be similar to that of *H. influenzae* type b strain Eagan (*7*). Two phosphate monoesters were found in the lipid A region, and a third phosphate group substituting the KDO. In addition, PEA was found to be on the O-6 position of HepII, as we previously demonstrated for strain Eagan (*7*). A LPS subpopulation was found to carry pyrophosphoethanolamine at the O-4 position of KDO (Table 1), depending on the method used for LPS isolation, while another contained only phosphomonoester.

Mild acid hydrolysis of the RM7004 LPS afforded a water soluble oligosaccharide fraction and nonsoluble lipid A. Two sharp ^{1}H resonances (2.18 and 3.23 ppm, 3H) were observed in the 1D ^{1}H NMR spectrum which were attributed to *O*-acetyl and phosphocholine (*P*Cho) substituents, respectively (*8*, *9*). The respective corresponding ^{13}C resonances were identified from an HMQC spectrum at 21.5 and 55.0 ppm. In the O-deacylated sample of LPS, the signal due to the *O*-acetyl group was absent. The ^{1}H and ^{13}C resonances typical of the *P*Cho groups were observed at 3.24 (δ_H) and 55.2 ppm (δ_C) in the O-deacylated LPS glycoform. We have previously reported the presence of *P*Cho groups in RM7004 LPS (*39*). Although *P*Cho was observed to be present in a very small amount (≈1%), its location was recently determined to be at the O-6 position of GalI in a *lic*2 mutant of RM7004 (*9*). Because of the high heterogeneity of the core OS sample obtained from the RM7004 LPS, it was not possible to determine the location of the *O*-acetyl groups. In the LPS of a related strain, *H. influenzae* strain Eagan, and its *lgtC* mutant (*17*), *O*-acetyl groups were found to be at the O-3 position of HepIII. This was determined from the relatively downfield shifted values for HepIII H-3 (5.03 ppm) as evidenced from the characteristic H-1 (5.08 ppm) → H-2 (4.19 ppm) → H-3 connectivity pathway in the COSY spectrum of a core oligosaccharide sample (unpublished data). On the basis of the genetic similarities of the two strains, we propose that the *O*-acetyl groups are located at the same position in the LPS of stain RM7004.

On the basis of the combined 2D NMR, ESI-MS, and methylation analyses, in conjunction with the previously reported LPS structure of the deep-rough chemotype from *H. influenzae* strain I-69 Rd$^-$/b$^+$ (*33*, *52*), the structures of the major LPS glycoforms or *H. influenzae* type b strain RM7004 are proposed in Figure 7.

DISCUSSION

In this study, the chemical structure of LPS from *H. influenzae* type b strain RM7004 was investigated and the detailed molecular structures of the major glycoform populations were elucidated (Figure 7). ESI-MS and NMR data indicated that all LPS glycoforms are related to one another by addition or deletion of hexose residues and/or PEA to or from a common basal unit. The basal unit was found to be composed of a heptose-containing trisaccharide which was linked to the lipid A via a phosphorylated KDO as observed in every strain of *H. influenzae* investigated to date (*6*−*10*). This basal structure has been found to be a common feature of LPS from *Haemophilus ducreyi* (*54*) and *Pasteurella* (*Manheimia*) *haemolytica* (*55*, *56*). Oligosaccharide extensions from the basal unit result in a complex mixture of isomeric glycoforms ranging from Hex3 to Hex9 in this strain of *H. influenzae*. A Hex6 glycoform having a tetrasaccharide extension from HepII was found to form the predominant LPS glycoform population, identical to an analogous LPS glycoform in strain Eagan (*7*). Sequential addition of hexose residues to the β-D-Glc*p* residue on HepI gives rise to the major population of Hex7−Hex9 glycoforms. Isomeric populations of glycoforms (representing an average of 40% of the total) in which HepIII is unsubstituted were also characterized (Hex3′−Hex8′ glycoforms). More extensive chain extension from HepI was particularly evident in this population of isomeric glycoforms. The gene involved in controlling glycan addition at HepIII (*lpsA*) has been identified (*15*, *17*). The Hex9 (Hex8′) glycoform showed two tetrasaccharide extensions on the first and second heptose residues (HepI and HepII). Both extensions contain the globoside trisaccharide (P^K antigen) α-D-Gal*p*-(1→4)-β-D-Gal*p*-(1→4)-β-D-Glc*p*, as a terminal unit. The expression of oligosaccharide extensions that mimic human blood group

Table 7: Structures of Major LPS Glycoforms of *H. influenzae* RM7004 Showing Heterogeneity Arising from Phase Variable Gene Expression

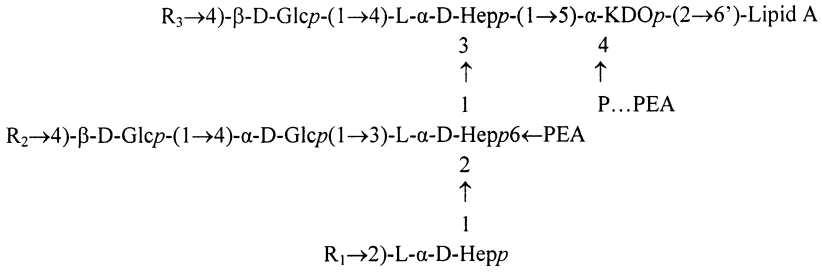

glycoform	R_1[a]	R_2	R_3	phase variable gene expression		
				lic2a	*lgtC*	*lex2*
Hex3	H	H	H	off	off	off
Hex4	β-D-Gal*p*	H	H	off	off	off
	H	β-D-Gal*p*	H	on	off	off
Hex5	β-D-Gal*p*	β-D-Gal*p*	H	on	off	off
	H	α-D-Gal*p*-(1→4)-β-D-Gal*p*	H	on	on	off
Hex6	β-D-Gal*p*	α-D-Gal*p*-(1→4)-β-D-Gal*p*	H	on	on	off
	H	α-D-Gal*p*-(1→4)-β-D-Gal*p*	β-D-Glc*p*	on	on	on
Hex7	β-D-Gal*p*	α-D-Gal*p*-(1→4)-β-D-Gal*p*	β-D-Glc*p*	on	on	on
	H	α-D-Gal*p*-(1→4)-β-D-Gal*p*	β-D-Gal*p*-(1→4)-β-D-Glc*p*	on	on	on
Hex8	β-D-Gal*p*	α-D-Gal*p*-(1→4)-β-D-Gal*p*	β-D-Gal*p*-(1→4)-β-D-Glc*p*	on	on	on
	H	α-D-Gal*p*-(1→4)-β-D-Gal*p*	α-D-Gal*p*-(1→4)-β-D-Gal*p*-(1→4)-β-D-Glc*p*	on	on	on
Hex9	β-D-Gal*p*	α-D-Gal*p*-(1→4)-β-D-Gal*p*	α-D-Gal*p*-(1→4)-β-D-Gal*p*-(1→4)-β-D-Glc*p*	on	on	on

[a] β-D-Gal*p* is transferred to the O-2 position of HepIII (R^1) by the *lpsA* gene (*17*). Expression of this gene is not regulated by phase variation. Although glycoforms containing β-D-Gal*p* at R^1 account for only ca. 70% of the isolated LPS, this may be due to donor availability or to steric effects, particularly in higher-molecular mass glycoforms (cf. Table 2).

antigens such as the P^K antigen is thought to provide a mechanism leading to an enhanced capacity for *H. influenzae* to evade host immune defenses (*12*, *13*). The globotriose terminal structure is also present in LPS of the closely related *H. influenzae* type b strain, Eagan (*7*), and nontypable strain SB33 (*10*), and in LPS species from *Neisseria meningitidis* L1 (*57*), *Neisseria gonorrheae* (*58*), and *Moraxella catarrhalis* (*28*, *59*). The isomeric distribution of glycoforms would suggest that addition of hexose residues during biosynthesis is highly regulated, where the elongation of hexose residues generally takes place on the central heptose before elongation of the β-D-Glc*p* on HepI occurs. The gene responsible for encoding the glycosyltransferase that initiates chain extension from the β-D-Glc*p* by addition of a second β-D-Glc*p* (*lex2*) was recently characterized (R. Aubrey et al., manuscript submitted for publication). It is possible that *lex2* is expressed at a later point in LPS biosynthesis, accounting for this observation. It is noteworthy that a nonfunctional *lex2* gene is present in strain Eagan (Aubrey et al., submitted) which is consistent with the absence of a globotriose extension from the glucose off HepI in LPS from that strain (*7*). In certain mutant strains of RM7004, a β-1,4-glucose disaccharide (cellobiose) extension has been observed at HepI irrespective of the degree of substitution at HepII. Thus, the major LPS glycoforms expressed by a *lic1*/*lic2* double mutant strain (AH1−3) carry a cellobiose unit from HepI with no substitution from HepII (*60*). In a *galE*/*galK* mutant, LPS glycoforms containing mono- and diglucoside extensions from HepI and HepII were observed (*61*). Glucose disaccharide branches were observed on both HepI and HepII in LPS from *H. influenzae* type b strain A2 (*40*).

Genes in the *lic2* locus in *H. influenzae* strain Rd and type b strains, Eagan and RM7004, have been implicated in the expression of the globotriose epitope (*15*, *17*, *19*). *lic2A* mediates the addition of UDP-galactose (UDP-Gal) to a β-D-Glc*p* acceptor to give lactose in the growing oligosaccharide chain. Recently, the gene product from *lgtC* in strain Eagan was shown to have α-galactosyltransferase activity (*17*), mediating the addition of UDP-Gal to lactose to give the globotriose unit. This gene is also present in strain RM7004 (*15*, *17*). Both *lic2A* and *lgtC* contain multiple, tandem tetranucleotide repeat motifs at the extreme 5′ end of the coding regions of the genes. Loss or gain of one or more of these tetranucleotide repeats, through a mechanism of slipped-strand miss pairing, shifts potential initiation codons in or out of frame with the remainder of the open reading frame, creating a translational switch, thus contributing to phase variable expression of the globotriose epitope. The effects of phase variable expression of *lex2*, *lic2A*, and *lgtC* on LPS globotriose expression and glycoform distribution are shown in Table 7.

It is interesting to note that the nine-carbon sugar acid neuraminic acid (sialic acid, Neu5Ac) has been detected as a component of the LPS in a majority of typable and nontypable strains of *H. influenzae* (*62*, *63*). Sialylation of *H. influenzae* LPS has been shown to increase the capacity of the organism to resist the bactericidal effects of human serum (*16*, *62*). LPS glycoforms containing sialyllactose and/or sialyllacto-*N*-neotetraose side chains have been structurally characterized, and at least three sialyltransferases have been described (*16*, *64*, *65*). Expression of sialylated LPS glycoforms would appear to depend on an exogenous source of sialic acid or its nucleotide-activated form, CMP-Neur5Ac (*16*, *66*). Sialic acid-containing glycoforms have previously been detected in *H. influenzae* LPS from serotype b strain A2 (*40*), and from strain Eagan (RM153) when it was grown under appropriate conditions, i.e., in the presence of Neu5Ac (D. W. Hood et al., manuscript in preparation). Interestingly,

it has been reported that the globotriose side chains of *N. meningitidis* immunotype L1 LPS can carry terminal sialic acid at the O-6 position of the α-D-Gal*p* residues (*67*). Under the growth conditions employed in the this investigation, we were unable to detect sialic acid-containing LPS glycoforms, indicating their absence or expression levels below the detection limits of the CE-ESI-MS techniques that were employed.

The phase variable gene, *lic3A*, has been shown to encode an α-2,3-sialyltransferase that mediates addition of Neu5Ac from CMP-Neu5Ac to a lactose extension in *H. influenzae* strain Rd as well as a wide range of nontypable strains (*16*). While RM7004 contains this gene, there is a single deletion of 141 base pairs downstream from the repeat region which could account for the lack of a sialyllactose-containing LPS phenotype (*16*).

To date, structural studies have indicated that LPS from all *H. influenzae* strains contain two phosphomonoester groups in the lipid A, phosphate, or pyrophosphoethanolamine at the O-4 position of KDO, and PEA at the O-6 position of HepII. Phosphomonoester groups were found to be at the O-4 position of HepIII in the Hex4 LPS glycoform of strain Eagan and its *lgt*C mutant (*7*; H. Masoud, D. Hood, E. R. Moxon, and J. C. Richards, unpublished result), while no phosphate groups were detected on HepIII in any of the LPS glycoforms of strain RM7004 (this study). Interestingly, PEA was found to substitute for the same heptose in LPS of nontypable *H. influenzae* strain 2019 (*43*). We have found PEA groups to be immunodominant epitopes that can evoke a functional IgG antibody in meningococcal lipopolysaccharide oligosaccharide (*68*, *69*). In *H. influenzae* LPS, PEA groups in the basal unit may provide unique epitopes for producing cross-reactive *H. influenzae* specific antisera or for development of LPS-based vaccine candidates. The presence of *P*Cho was detected in RM7004 LPS to the extent of 1−2% by ^{1}H NMR. The level of expression could be enriched by selecting for *lic1* phase-on variants when the organisms were grown on solid media (*9*, *39*). The *P*Cho groups were determined to be at the O-6 position of the β-D-Gal*p* on the distal heptose of the basal unit in a *lic2* mutant strain (*9*). *P*Cho has been detected as a major component in *H. influenzae* strain RM118 (Rd) (*8*). It is noteworthy that the location of *P*Cho in strain RM118 is at the O-6 position of the β-Glc*p* on the first heptose.

The presence of *O*-acetyl groups was also identified in the LPS of *H. influenzae* RM7004. The *O*-acetyl group was found to be attached at the O-3 position of HepIII in the wild type and *lgt*C mutant of strain Eagan (H. Masoud, D. Hood, E. R. Moxon, and J. C. Richards, unpublished result), and we assume it to be at the same position in strain RM7004.

ACKNOWLEDGMENT

We thank D. Griffith for large-scale production of cells, R. A. Z. Johnston for GLC−MS analysis, and D. Krajcarski for ESI-MS analysis.

REFERENCES

1. Robbins, J. B., Schneerson, R., Argaman, M., et al. (1973) *Ann. Intern. Med. 78*, 259−269.
2. Zwahlen, A., Rubin, L. G., Connelly, C. J., Inzana, T. J., and Moxon, E. R. (1990) *J. Infect. Dis. 152*, 485−492.
3. Turk, D. C. (1981) in *Haemophilus influenzae: Epidemiology, Immunology and Prevention of Disease* (Sell, S. H., and Wright, P. F., Eds.) pp 3−9, Elsevier, New York.
4. Moxon, E. R., and Vaughn, K. A. (1981) *J. Infect. Dis. 143*, 517−524.
5. Gibson, B. W., Phillips, N. J., Melaugh, W., and Engstrom, J. J. (1996) In *Biochemical and Biotechnological Application of Electrospray Ionization Mass Spectrometry* (Snyder, A. P., Ed.) pp 166−184, American Chemical Society, Washington, DC.
6. Månsson, M., Bauer, S. H., Hood, D. W., Richards, J. C., Moxon, E. R., and Schweda, E. K. (2001) *Eur. J. Biochem. 268*, 2148−2159.
7. Masoud, H., Moxon, E. R., Martin, A., Krajcarski, D., and Richards, J. C. (1997) *Biochemistry 36*, 2091−2103.
8. Risberg, A., Masoud, H., Martin, A., Richards, J. C., Moxon, E. R., and Schweda, E. K. H. (1999) *Eur. J. Biochem. 261*, 171−180.
9. Schweda, E. K. H., Brisson, J.-R., Alvelius, G., Martin, A., Weiser, J. N., Hood, D. W., Moxon, E. R., and Richards, J. C. (2000) *Eur. J. Biochem. 267*, 3902−3913.
10. Cox, A. D., Masoud, H., Thibault, P., Brisson, J.-R., van der Zwan, M., Li, J., Perry, M. B., and Richards, J. C. (2001) *Eur. J. Biochem. 268*, 5278−5286.
11. Abu Kwaik, Y., Lesse, A., Yamasaki, R., Gibson, B., Spinola, S. M., and Apicella, M. A. (1992) *Infect. Immun. 60*, 1322−1328.
12. Weiser, J. N., Williams, A., and Moxon, E. R. (1990) *Infect. Immun. 58*, 3455−3457.
13. Weiser, J. N. (1993) *J. Infect. Dis. 168*, 672−680.
14. Weiser, J. N., Love, J., and Moxon, E. R. (1989) *Cell 59*, 657−665.
15. Hood, D. W., Deadman, M. E., Allen, T., Masoud, H., Martin, A., Brisson, J.-R., Fleischmann, R., Venter, J. C., Richards, J. C., and Moxon, E. R. (1996) *Mol. Microbiol. 22*, 951−965.
16. Hood, D. W., Cox, A. D., Gilbert, M., Makepeace, K. M., Walsh, S., Deadman, M. E., Cody, A., Martin, A., Månsson, M., Schweda, E. K. H., Brisson, J.-R., Richards, J. C., Moxon, E. R., and Wakarchuk, W. W. (2001) *Mol. Microbiol. 39*, 341−350.
17. Hood, D. W., Cox, A., Wakarchuck, W., Schur, M., Scweda, E., Walsh, S. L., Deadman, M., Martin, A., Moxon, R. E., and Richards, J. C. (2001) *Glycobiology 11*, 957−967.
18. Virgi, M., Weiser, J. W., Lindberg, A. A., and Moxon, E. R. (1990) *Microbiol. Pathol. 9*, 441−450.
19. High, N. J., Deadman, M. E., and Moxon, E. R. (1993) *Mol. Microbiol. 9*, 1275−1278.
20. Karlsson, K. A., Bock, K., Strombert, N., and Teneberg, S. (1986) in *Protein-Carbohydrate Interactions* (Lark, D. L., Ed.) pp 207−203, Academic Press, London.
21. Van Alphen, L., Riemans, T., Poolman, J., Hopman, C., and Zanen, H. C. (1983) *J. Infect. Dis 148*, 75−81.
22. Westphal, O., Lüderitz, O., and Bister, F. (1952) *Z. Naturforsch. 7b*, 148−155.
23. Laemmli, U. K., and Favre, M. (1973) *J. Mol. Biol. 80*, 575−599.
24. Komuro, T., and Galanos, C. (1988) *J. Chromatogr. 450*, 381−387.
25. Tsai, C.-M., and Frasch, C. E. (1982) *Anal. Biochem. 119*, 115−119.
26. Holst, O., Brade, L., Kosma, P., and Brade, H. (1991) *J. Bacteriol. 173*, 1862−1866.
27. Masoud, H., Altman, E., Richards, J. C., and Lam, J. S. (1994) *Biochemistry 33*, 10568−10578.
28. Masoud, H., Perry, M. B., Brisson, J.-R., Uhrin, D., and Richards, J. C. (1994) *Can. J. Chem. 72*, 1466−1477.
29. Dubois, M., Gilles, K. A., Hamilton, J. K., Rebers, P. A., and Smith, F. (1956) *Anal. Chem. 28*, 350−356.
30. York, W. S., Darvill, A. G., McNeil, M., Stevenson, T. T., and Albersheim, P. (1985) *Methods Enzymol. 118*, 3−40.
31. Coleman, W. G., Jr. (1983) *J. Biol. Chem. 258*, 1985−1990.
32. Gerwig, G. J., Kamerling, J. P., and Vliegenthart, J. F. G. (1979) *Carbohydr. Res. 77*, 1−7.
33. Helander, I. M., Lindner, B., Brade, H., Altmann, K., Lindberg, A. A., Rietschel, E. Th., and Zähringer, U. (1988) *Eur. J. Biochem. 177*, 483−492.
34. Hakomori, H. I. (1964) *J. Biochem. 55*, 205−208.
35. Mort, A. J., Parker, S., and Kuo, M.-S. (1983) *Anal. Biochem. 133*, 380−384.
36. Stellner, K., Saito, H., and Hakomori, S. I. (1973) *Arch. Biochem. Biophys. 155*, 464−472.

37. Shaka, A. J., Keeler, J., Frenkiel, F., and Freeman, R. (1983) *J. Magn. Reson. 52*, 335−338.
38. Thibault, P., Li, J., Martin, A., Richards, J. C., Hood, D. W., and Moxon, E. R. (1999) in *Mass Spectrometry in Medicine and Biology* (Burlingame, S., Carr, M. T., and Bowers, Eds.) pp 439−462, Humana Press, Totowa, NJ.
39. Weiser, J. N., Pan, N., McGowan, K. L., Musher, D., Martin, A., and Richards, J. C. (1998) *J. Exp. Med. 187*, 631−640.
40. Phillips, N. J., Apicella, M. A., Griffiss, J. M., and Gibson, B. W. (1993) *Biochemistry 32*, 2003−2012.
41. Gibson, B. W., Melaugh, W., Phillips, N. J., Apicella, M. A., Campagnari, A. A., and Griffiss, J. M. (1993) *J. Bacteriol. 175*, 2702−2712.
42. Phillips, N. J., McLaughlin, R., Miller, T. J., Apicella, M. A., and Gibson, B. W. (1996) *Biochemistry 35*, 5937−5947.
43. Phillips, N. J., Apicella, M. A., Griffiss, J. M., and Gibson, B. W. (1992) *Biochemistry 31*, 4515−4526.
44. Bock, K., and Thøgerssen, H. (1982) *Annu. Rep. NMR Spectrosc. 13*, 1−57.
45. Altona, C., and Haasnoot, C. A. G. (1980) *Org. Magn. Reson. 13*, 417−429.
46. Bock, K., and Pedersen, C. (1983) *Adv. Carbohydr. Chem. Biochem. 41* 27−66.
47. Bock, K., Pedersen, C., and Pedersen, H. (1984) *Adv. Carbohydr. Chem. Biochem. 42*, 193−225.
48. Unger, F. M. (1981) *Carbohydr. Chem. Biochem. 38*, 323−388.
49. York, W. S., Darvill, A. G., McNeil, M., and Albersheim, P. (1985) *Carbohydr. Res. 138*, 190−126.
50. Carlson, R. W., Hollingsworth, R. L., and Dazzo, F. B. (1988) *Carbohydr. Res. 176*, 127−135.
51. Richards, J. C., and Perry, M. B. (1988) *Biochem. Cell Biol. 66*, 758−771.
52. Zamze, S. E., Ferguson, M. A. J., Moxon, E. R., Owek, R. A., and Rademacher, T. W. (1987) *Biochem. J. 245*, 583−587.
53. Dabrowski, J. (1989) *Methods Enzymol. 179*, 122−156.
54. Schweda, E. K. H., Sundström, A. C., Eriksson, L. M., Jonasson, J. A., and Lindberg, A. A. (1994) *J. Biol. Chem. 269*, 12040−12048.
55. Severn, W. B., Johnston, R. A. Z., Kelly, R. F., and Richards, J. C. (1994) The structural analysis of short chain lipopolysaccharide, *XVIIth International Carbohydrate Symposium*, July 17−22, Ottawa, ON.
56. Brisson, J.-R., Crawford, E., Dušan, U., Khieu, N. H., Perry, M. B., Severn, W. B., and Richards, J. C. (2002) *Can. J. Chem. 80*, 1−15.
57. DiFabio, J. L., Michon, F., Brisson, J.-R., and Jennings, H. J. (1990) *J. Biol. Chem. 265*, 7243−7247.
58. John, C. M., Griffiss, J. M., Apicella, M. A., Mandrell, R. E., and Gibson, B. W. (1991) *J. Biol. Chem. 266*, 19303−19311.
59. Edebrink, P., Jansson, P.-E., Rahman, M. M., Widmalm, G., Holme, T., and Weintraub, A. (1994) *Carbohydr. Res. 257*, 269−284.
60. Schweda, E. K. H., Hegedus, O. E., Borrelli, S., Lindberg, A. A., Weiser, J. N., Maskell, D. J., and Moxon, E. R. (1993) *Carbohydr. Res. 246*, 319−330.
61. Schweda, E. K. H., Jansson, P.-E., Moxon, E. R., and Lindberg, A. A. (1995) *Carbohydr. Res. 272*, 213−224.
62. Hood, D. W., Makepeace, K. M., Deadman, M. E., Rest, R. F., Thibault, P., Martin, A., Richards, J. C., and Moxon, E. R. (1999) *Mol. Microbiol. 33*, 679−692.
63. Bauer, S. H. J., Månsson, M., Hood, D. W., Richards, J. C., Moxon, E. R., and Schweda, E. K. H. (2001) *Carbohydr. Res. 335*, 251−260.
64. Cox, A. D., Hood, D. W., Martin, A., Makepeace, K. M., Deadman, M. E., Li, J., Brisson, J.-R., Moxon, E. R., and Richards, J. C. (2002) *Eur. J. Biochem. 269*, 4009−4019.
65. Jones, P. A., Samuels, N. M., Phillips, N. J., Muson, R. S., Jr., Bozue, J. A., Arseneau, J. A., Nichols, W. A., Zaleski, A., Gibson, B. W., and Apicella, M. A. (2002) *J. Biol. Chem. 277*, 14598−14611.
66. Vimr, E., Lichtensteiger, C., and Steenbergen, S. (2000) *Mol. Microbiol. 36*, 289−293.
67. Wakarchuk, W. W., Gilbert, M., Martin, A., Wu, Y., Brisson, J.-R., Thibault, P., and Richards, J. C. (1998) *Eur. J. Biochem. 254*, 626−633.
68. Plested, J. S., Makepeace, K., Jennings, M. P., Gidney, M. A. J., Lacelle, S., Brisson, J.-R., Cox, A. D., Martin, A., Bird, A. G., Tang, J. C., MacKinnon, F. M., Richards, J. C., and Moxon, E. R. (1999) *Infect. Immun. 67*, 5417−5426.
69. Plested, J. S., Ferry, B. L., Coull, P. A., Makepeace, K., Lehmann, A. K., MacKinnon, F. G., Griffiths, H. G., Herbert, M. A., Richards, J. C., and Moxon, E. R. (2001) *Infect. Immun. 69*, 3203−3213.

BI026632A